FINITE ELEMENT MODELING OF WOOD DIAPHRAGMS

By Robert H. Falk[1] and Rafii Y. Itani,[2] Member, ASCE

ABSTRACT: This report describes a two-dimensional finite element model for analyzing vertical and horizontal wood diaphragms. Central to the development of this model is the formulation of a nonlinear finite element that accounts for the distribution and stiffness of fasteners connecting the sheathing to the framing. Linked with conventional beam and plane stress elements, which represent diaphragm framing and sheathing, respectively, the resulting model can be used to analyze a variety of wood diaphragms (walls, floors. ceilings, etc.). Load-displacement results from experimentally tested diaphragms and model predictions were found to be in good agreement. Parametric studies with the model show that diaphragm stiffness is significantly affected by nail stiffness, nail spacing, and the use of blocking. At code allowable diaphragm shear load levels, a variation of 20% in nail stiffness resulted in a change in diaphragm stiffness of less than 10%. Nail spacing was shown to have a more dominant effect on diaphragm stiffness than nail stiffness.

INTRODUCTION

Diaphragms are important components of wood-framed buildings that are used to resist and transfer the lateral shear forces produced by wind or earthquakes. The analysis of these complex components has been oversimplified because of a lack of understanding of their static and dynamic behavior. Analytical research efforts have primarily concentrated on the modeling of wall diaphragm behavior. Few models have been used to address the behavior of other types of diaphragms, such as floors and ceilings.

The purpose of this paper is to describe a nonlinear finite element formulated to represent the distribution and stiffness of the nails that secure sheathing to framing in a wood diaphragm. When linked with conventional beam and plane stress elements, which represent diaphragm framing and sheathing, respectively, the resulting model can be used to analyze a variety of diaphragms (walls, floors, and ceilings) with different geometry and loading arrangements.

We also present the results of studies performed with the developed model to determine the effect of varying input parameters — nail properties, nail spacing, and the use of blocking—on floor diaphragms.

RELATED RESEARCH

Though research on wood diaphragms dates back to 1927 (Peterson 1983), most of the research until the 1960s was experimental in nature and focused

[1]Res. Engr., Forest Prod. Lab., Forest Serv., U.S. Dept. of Agric., One Gifford Pinchot Drive, Madison, WI 53705-2398; formerly, Grad. Student, Dept. of Civ. and Environ. Engrg., Washington State Univ., Pullman, WA 99164-2914. The Forest Products Laboratory is maintained in cooperation with the University of Wisconsin.

[2]Prof., Civ. and Environ. Engrg., Washington State University, Pullman, WA 99164–2914.

Note. Discussion open until August 1, 1989. To extend the closing date one month, a written request must be filed with the ASCE Manager of Journals. The manuscript for this paper was submitted for review and possible publication on January 15, 1988. This paper is part of the *Journal of Structural Engineering,* Vol. 115, No. 3, March, 1989. ASCE, Paper No. 23247.

on the relative influence of parameters such as sheathing type and orientation, fastener type and spacing, and diaphragm geometry. Several mathematical models for wood diaphragm analysis have since been proposed. In 1967, Amana and Booth published the results of theoretical studies on nailed and glued plywood stressed skin components. The concept of nail modulus used to account for fastener stiffness was first presented in this paper. Foschi presented a more general nonlinear finite element model in 1977 that was used to predict the displacements of a 20 by 60 ft roof diaphragm. Utilizing a connector element, which accounted for a single line of fasteners, good agreement was obtained between the model and the test diaphragm. In 1978, Tuomi and McCutcheon described a theoretical model for predicting racking resistance of wood stud walls. Experimental test data and theoretical results were in good agreement. Although this model was limited to linear nail joint slip, it has since been modified to account for fastener nonlinearity (McCutcheon 1985).

Formulas for analyzing wood-frame shear walls with sheathing attached by discrete fasteners were presented by Easley et al. in 1982. Expressions were derived for sheathing fastener forces, linear shear stiffness, and nonlinear shear load-strain behavior. These formulas were shown to be in agreement with a finite element analysis and with the results of wall racking tests. Eight 8 by 12 ft plywood-sheathed walls were tested for model verification.

In 1983, Kamiya et al. used a previously developed procedure (Kamiya 198 1) to predict the performance of wood-sheathed walls. Single-nail joints were tested to obtain load-slip characteristics needed for analysis. This simplified procedure predicted allowable shear loads for various wall constructions. In Sweden during the same year, Kallsner (1983) also presented a simplified wood shear wall model that was based upon the principle of minimum potential energy. Coupon testing of various fasteners as well as full-scale wall tests were performed. The theoretical model predicted wall load capacity to within 20% of measured values.

A more recent model for simplifying wall diaphragm analysis was proposed by Gupta and Kuo in 1985. This strain energy approach models nonlinear behavior, and does not need the closed-form equations present in some previous models. Modification of this model has provided for the effects of shear wall uplift (Gupta and Kuo 1987).

Itani and Cheung presented a finite element model in 1984 for the static analysis of wood diaphragms. A single line of fasteners could be represented with the developed joint element, which accounted for nonlinear nail slip properties. This model does not impose restrictions on sheathing arrangement, load application, or diaphragm geometry. Analysis with this model, however, indicated that an excessive number of structural degrees of freedom (DOF) were required to model larger diaphragms. It was clear that a model requiring fewer DOF and a better representation of the distributed fasteners was needed if larger ceiling and floor diaphragms were to be practically analyzed. The model described in this paper is the result.

FINITE ELEMENT FORMULATION

Wood diaphragms are constructed from three basic elements: frame members (studs or joists), sheathing (plywood, particleboard, or gypsumboard),

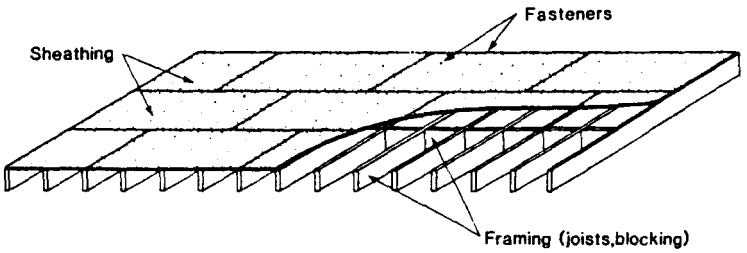

FIG. 1. Typical Floor Diaphragm

and fasteners (nails or staples). Fig. 1 shows a typically constructed floor diaphragm. The finite element developed in the following formulation represents the distribution and stiffness of nail fasteners connecting sheathing panels and lumber framing in a wall, floor, ceiling, or roof diaphragm. This element will be referred to as a "transfer element" since it accounts for the transfer of lateral force through the fasteners from the sheathing to the framing (and vice versa).

The transfer element accounts for the stiffness of individual fasteners through the use of spring pairs, which can deform nonlinearly (Easley et al. 1982). Fig. 2 shows a spring pair in the undeformed state. The spring pair represents the lateral stiffness of an individual nail, which is determined from experimental tests of single nail joints. Linking of the transfer element with conventional beam and plane stress isoparametric elements, which are used to model the lumber framing and sheathing panels, respectively, allows analysis of an entire diaphragm subject to lateral loads.

The transfer element accounts for the distribution of multiple nails securing sheathing panels to the framing as well as the nonlinear stiffness of each

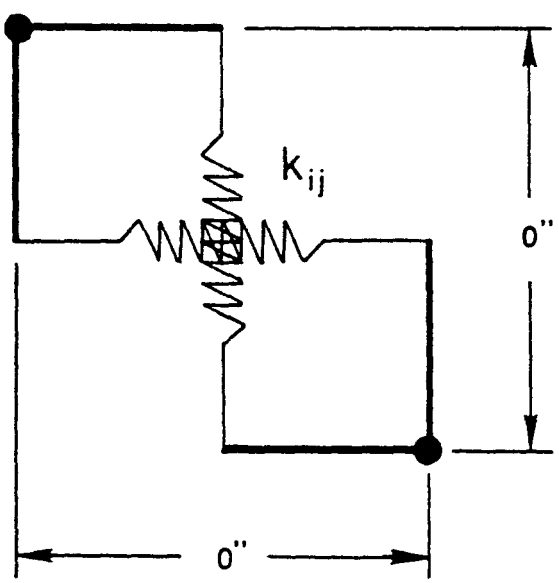

FIG. 2. Undeformed Spring Pair

nail resulting from the relative displacement of the framing and sheathing. The stiffness matrix of the transfer element is established through a summation of the stiffnesses of the individual fasteners. Typically, a transfer element is sized to match the dimensions of the sheathing element to which it connects (accounting for all the fasteners connecting that sheathing panel to the framing).

Since the transfer element is linked between a single sheathing element and at least four beam elements, the number of nodes and the resulting number of DOF needed to describe the transfer element are dictated only by its connection to these elements, not by the number of fasteners it represents. Previous formulations were dependent on a description of a single fastener or a single line of fasteners (Easley et al. 1982; Foschi 1977; Itani and Cheung 1984). The representation of multiple rows and columns of fasteners by a single transfer element significantly reduces the DOF required for diaphragm analysis. A comparative analysis with the Itani and Cheung (1984) model indicated a 40% reduction in system DOF using the transfer element model, without significantly increasing the computational difficulty at the element level.

Fig. 3 shows the node numbers, DOF, and coordinate orientation of the transfer element. Height (H) and width (W) are variables dependent on the dimensions of the attached sheathing element. Though offset in the figure for clarity, nodes 1 to 4 have the same undisplaced coordinates as nodes 5 to 8, respectively. Nodes 1 to 4 link to beam elements, and nodes 5 to 8 link to the single sheathing element. Since beam elements possess 3 DOF per node and the plane stress isoparametric element used to model the sheathing possesses 2 DOF per node, the transfer element requires a total of 20 DOF.

The magnitude of spring pair displacement depends on their location in the element and the relative displacement of the beam and sheathing elements to which the transfer element is attached. The spring pairs have zero length before displacement (see Fig. 2).

Fig. 4 shows the displacement of spring pairs (only four shown for clarity) due to a unit displacement at DOF 1 (node 1) of the transfer element. The dashed lines indicate the location of the attached sheathing element, and the solid lines indicate the locations of the attached beam elements. The relative displacement of these solid and dashed lines define spring pair displacement. To assure compatibility, the functions describing the shape of the deformed dashed and solid lines are identical to the functions used to describe the beam and sheathing elements attached to the transfer element (see Table 1).

For example. $d_{1x}(y)$ describes the solid (beam) line as a result of displacement at node 1 in the x direction. The terms a_j in the tabulated functions indicate the location of spring pairs as a ratio of their y coordinate and element height (H) (Table 1, column 1).

Since the expressions d_{1x}, through d_{8y} can be used only to describe the displacement of spring pairs along the edges of the element, similar functions are also needed to describe spring pair displacement in the field of the element. These functions, c_{1x} - c_{8y}, are given in column 2 of Table 1. The terms b_i in the tabulated functions describe the x coordinate of spring pairs as a ratio of element width (W).

The terms "a_j" and "b_i" are used to define the location of spring pair ij anywhere on the x-y plane of the transfer element. Nails on the perimeter

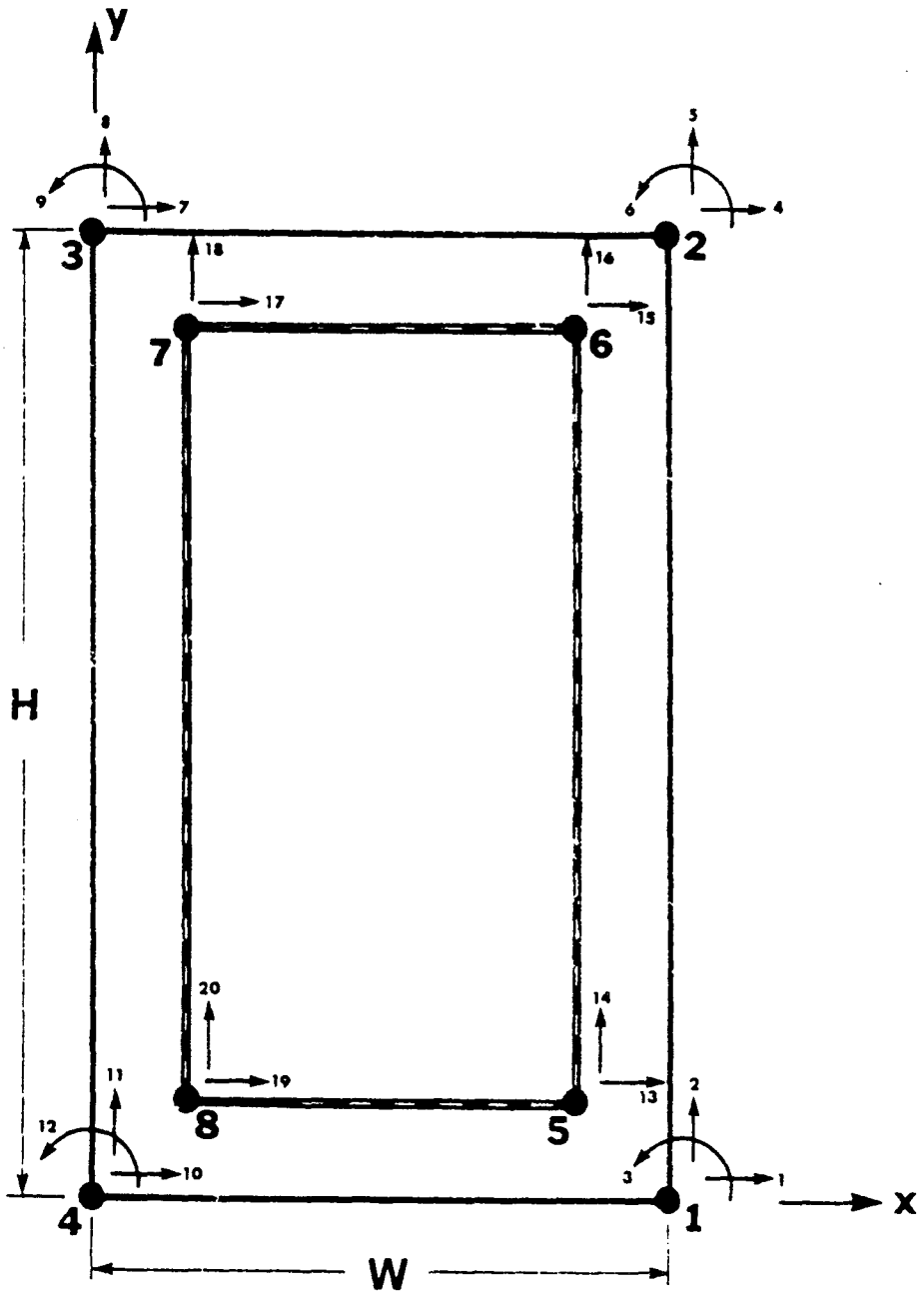

FIG. 3. Transfer Element. Nodes (1–8),Degree of Freedom (DOF), and Coordinate Orientation. *H*, Height; *W*, Width

of sheathing panels as well as interior (field) nails with different spacings can be represented.

To develop the stiffness matrix of the transfer element, unit displacements are successively applied to each DOF. Each spring pair displaces due to this model displacement and the resulting forces are summed to obtain the coef-

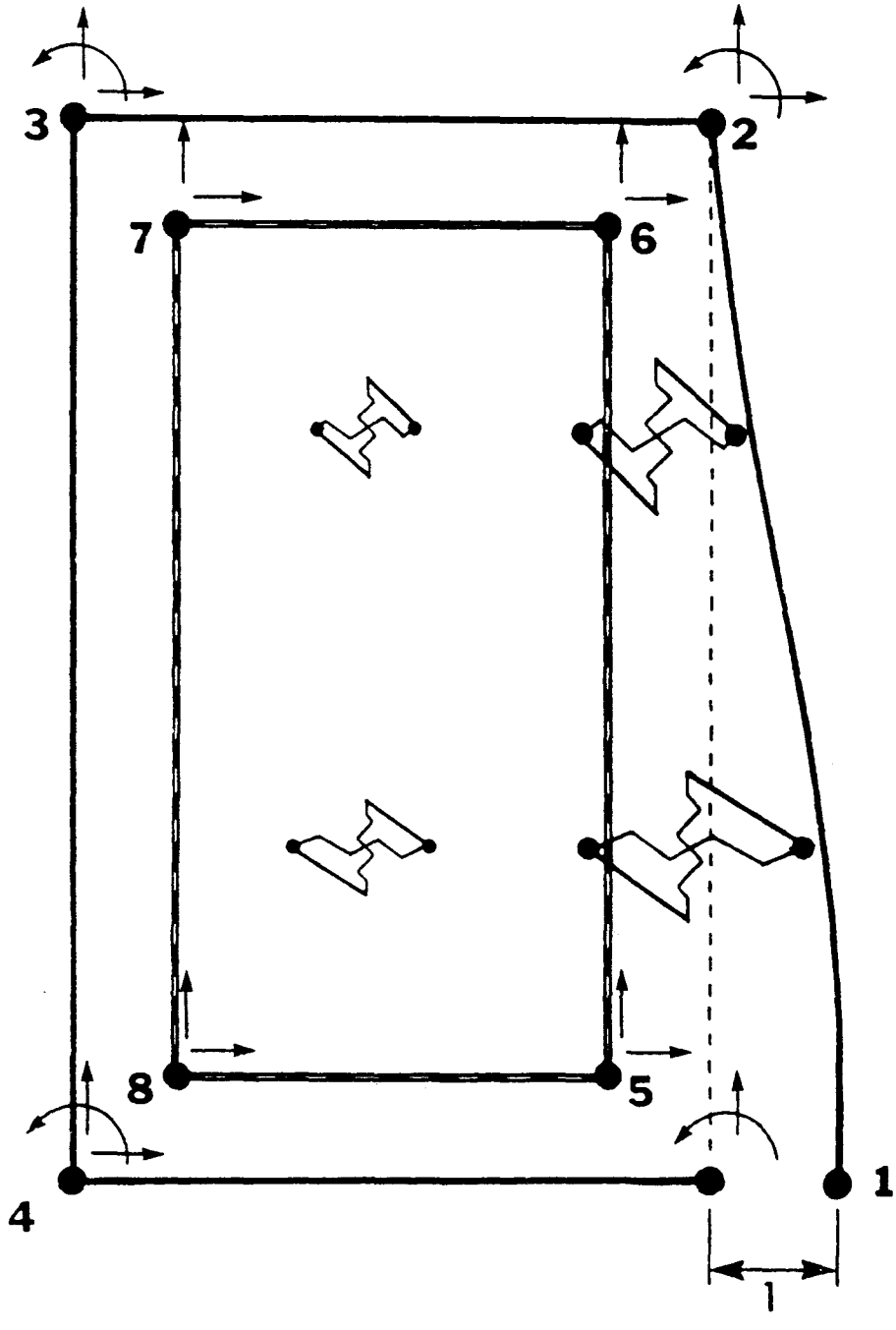

FIG. 4. Unit Displacement of Transfer Element at DOF 1 and Resulting Spring Pair Elongation

TABLE 1. Functions Describing Spring Pair Displacement

Displacement in terms of element height (1)	Displacement in terms of element width (2)
$d_{1x}(y) = 1 - 3a_j^2 + 2a_j^3$	$c_{1x}(x) = b_i$
$d_{1y}(y) = 1 - 3a_j^2 + 2a_j^3$	$c_{1y}(x) = b_i$
$d_{1\theta}(y) = [-a_j + 2a_j^2 - a_j^3]H$	$c_{1\theta}(x) = b_i$
$d_{2x}(y) = 3a_j^2 - 2a_j^3$	$c_{2x}(x) = b_i$
$d_{2y}(y) = 3a_j^2 - 2a_j^3$	$c_{2y}(x) = b_i$
$d_{2\theta}(y) = a_j^2 - a_j^3$	$c_{2\theta}(x) = b_i$
$d_{3x}(y) = 3a_j^2 - 2a_j^3$	$c_{3x}(x) = 1 - b_i$
$d_{3y}(y) = 3a_j^2 - 2a_j^3$	$c_{3y}(x) = 1 - b_i$
$d_{3\theta}(y) = a_j^2 - a_j^3$	$c_{3\theta}(x) = 1 - b_i$
$d_{4x}(y) = 1 - 3a_j^2 + 2a_j^3$	$c_{4x}(x) = 1 - b_i$
$d_{4y}(y) = 1 - 3a_j^2 + 2a_j^3$	$c_{4y}(x) = 1 - b_i$
$d_{4\theta}(y) = [-a_j + 2a_j^2 - a_j^3]H$	$c_{4\theta}(x) = 1 - b_i$
$d_{5x}(y) = 1 - a_j$	$c_{5x}(x) = b_i$
$d_{5y}(y) = 1 - a_j$	$c_{5y}(x) = b_i$
$d_{6x}(y) = a_j$	$c_{6x}(x) = b_i$
$d_{6y}(y) = a_j$	$c_{6y}(x) = b_i$
$d_{7x}(y) = 1 - a_j$	$c_{7x}(x) = 1 - b_i$
$d_{7y}(y) = 1 - a_j$	$c_{7y}(x) = 1 - b_i$
$d_{8x}(y) = a_j$	$c_{8x}(x) = 1 - b_i$
$d_{8y}(y) = a_j$	$c_{8y}(x) = 1 - b_i$

Note: $a_j = y/H$, where j indicates the jth spring pair in a column. $b_i = x/W$, where i indicates the ith spring pair in a row.

ficients of the transfer element stiffness matrix.

To determine the force at each spring, the displacement of the spring must be known (from Table 1 functions) and its nonlinear stiffness (k_{ij}, from experimental nail tests). The spring force associated with each spring pair is then obtained as a product of the nonlinear spring stiffness k_{ij} and the corresponding spring displacement. For example, the force f in spring pair ij, caused by a unit displacement at node 1 in the x direction, is expressed as

$$f_{1x,ijx} = k_{ij} d_{1x} c_{1x} \quad (1)$$

The subscripts of f indicate the node number and the direction of the unit displacement ($1x$) as well as the spring location and the component of force (ijx).

To determine the coefficients of the transfer element stiffness matrix, the resultant spring pair force at each DOF caused by unit displacement at each node must be determined. This nodal force, S, is equal to the sum of the product of the force in each spring pair and the corresponding function value describing spring pair displacement. This product describes the portion of each spring pair force distributed to each node. For example, the resultant force at node 2 in the x direction, caused by unit displacement applied at node 1 in the x direction, is expressed as

$$S_{2x,1x} = \sum_{i=1}^{n} \sum_{j=1}^{m} f_{1x,ijx} d_{2x} c_{2x} \quad (2)$$

Note that the total number of spring pairs in the *x*-*y* plane are represented by *n* and *m* (columns and rows), respectively. Substituting the expression for spring force (Eq. 1) into Eq. 2 gives

$$S_{2x,1x} = \sum_{i=1}^{n} \sum_{j=1}^{m} k_{ij} d_{1x} c_{1x} d_{2x} c_{2x} \quad \text{(3)}$$

The subscripts of *S* indicate the node and the direction of the resultant force (2*x*) and the node and direction of unit displacement (l*x*).

These resultant forces are computed by applying unit displacements at each DOF in turn, which produces a 20 by 20 stiffness matrix. Each resultant force *S* is a coefficient of this matrix as shown in Eq. 4.

The transfer element has been incorporated into a modified version of the computer program NONSAP (Cheung 1984). Input requires a description of nail location (*ij*) and an experimental nail load-slip curve from which k_{ij} can be determined.

$K_s = \sum_{ij} k_s$ (4)

$d_{1x}^2c_{1x}^2$	0	$d_{1x}d_{1\theta}c_{1x}c_{1\theta}$	$d_{1x}d_{2x}c_{1x}c_{2x}$	0	$d_{1x}d_{2\theta}c_{1x}c_{2\theta}$	$d_{1x}d_{3x}c_{1x}c_{3x}$	0	$d_{1x}d_{3\theta}c_{1x}c_{3\theta}$	$d_{1x}d_{4x}c_{1x}c_{4x}$	0	$d_{1x}d_{4\theta}c_{1x}c_{4\theta}$	$d_{1x}d_{5x}c_{1x}c_{5x}$	0	$d_{1x}d_{6x}c_{1x}c_{6x}$	0	$d_{1x}d_{7x}c_{1x}c_{7x}$	0	$d_{1x}d_{8x}c_{1x}c_{8x}$	0
	$d_{1y}^2c_{1y}^2$	0	0	$d_{1y}d_{2y}c_{1y}c_{2y}$	0	0	$d_{1y}d_{3y}c_{1y}c_{3y}$	0	0	$d_{1y}d_{4y}c_{1y}c_{4y}$	0	0	$d_{1y}d_{5y}c_{1y}c_{5y}$	0	$d_{1y}d_{6y}c_{1y}c_{6y}$	0	$d_{1y}d_{7y}c_{1y}c_{7y}$	0	$d_{1y}d_{8y}c_{1y}c_{8y}$
		$d_{1\theta}^2c_{1\theta}^2$	$d_{1\theta}d_{2x}c_{1\theta}c_{2x}$	0	$d_{1\theta}d_{2\theta}c_{1\theta}c_{2\theta}$	$d_{1\theta}d_{3x}c_{1\theta}c_{3x}$	0	$d_{1\theta}d_{3\theta}c_{1\theta}c_{3\theta}$	$d_{1\theta}d_{4x}c_{1\theta}c_{4x}$	0	$d_{1\theta}d_{4\theta}c_{1\theta}c_{4\theta}$	$d_{1\theta}d_{5x}c_{1\theta}c_{5x}$	0	$d_{1\theta}d_{6x}c_{1\theta}c_{6x}$	0	$d_{1\theta}d_{7x}c_{1\theta}c_{7x}$	0	$d_{1\theta}d_{8x}c_{1\theta}c_{8x}$	0
			$d_{2x}^2c_{2x}^2$	0	$d_{2x}d_{2\theta}c_{2x}c_{2\theta}$	$d_{2x}d_{3x}c_{2x}c_{3x}$	0	$d_{2x}d_{3\theta}c_{2x}c_{3\theta}$	$d_{2x}d_{4x}c_{2x}c_{4x}$	0	$d_{2x}d_{4\theta}c_{2x}c_{4\theta}$	$d_{2x}d_{5x}c_{2x}c_{5x}$	0	$d_{2x}d_{6x}c_{2x}c_{6x}$	0	$d_{2x}d_{7x}c_{2x}c_{7x}$	0	$d_{2x}d_{8x}c_{2x}c_{8x}$	0
				$d_{2y}^2c_{2y}^2$	0	0	$d_{2y}d_{3y}c_{2y}c_{3y}$	0	0	$d_{2y}d_{4y}c_{2y}c_{4y}$	0	0	$d_{2y}d_{5y}c_{2y}c_{5y}$	0	$d_{2y}d_{6y}c_{2y}c_{6y}$	0	$d_{2y}d_{7y}c_{2y}c_{7y}$	0	$d_{2y}d_{8y}c_{2y}d_{8y}$
					$d_{2\theta}^2c_{2\theta}^2$	$d_{2\theta}d_{3x}c_{2\theta}c_{3x}$	0	$d_{2\theta}d_{3\theta}c_{2\theta}c_{3\theta}$	$d_{2\theta}d_{4x}c_{2\theta}c_{4x}$	0	$d_{2\theta}d_{4\theta}c_{2\theta}c_{4\theta}$	$d_{2\theta}d_{5x}c_{2\theta}c_{5x}$	0	$d_{2\theta}d_{6x}c_{2\theta}c_{6x}$	0	$d_{2\theta}d_{7x}c_{2\theta}c_{7x}$	0	$d_{2\theta}d_{8x}c_{2\theta}c_{8x}$	0
						$d_{3x}^2c_{3x}^2$	0	$d_{3x}d_{3\theta}c_{3x}c_{3\theta}$	$d_{3x}d_{4x}c_{3x}c_{4x}$	0	$d_{3x}d_{4\theta}c_{3x}c_{4\theta}$	$d_{3x}d_{5x}c_{3x}c_{5x}$	0	$d_{3x}d_{6x}c_{3x}c_{6x}$	0	$d_{3x}d_{7x}c_{3x}c_{7x}$	0	$d_{3x}d_{8x}c_{3x}c_{8x}$	0
							$d_{3y}^2c_{3y}^2$	0	0	$d_{3y}d_{4y}c_{3y}c_{4y}$	0	0	$d_{3y}d_{5y}c_{3y}c_{5y}$	0	$d_{3y}d_{6y}c_{3y}c_{6y}$	0	$d_{3y}d_{7y}c_{3y}c_{7y}$	0	$d_{3y}d_{8y}c_{3y}c_{8y}$
								$d_{3\theta}^2c_{3\theta}^2$	$d_{3\theta}d_{4x}c_{3\theta}c_{4x}$	0	$d_{3\theta}d_{4\theta}c_{3\theta}c_{4\theta}$	$d_{3\theta}d_{5x}c_{3\theta}c_{5x}$	0	$d_{3\theta}d_{6x}c_{3\theta}c_{6x}$	0	$d_{3\theta}d_{7x}c_{3\theta}c_{7x}$	0	$d_{3\theta}d_{8x}c_{3\theta}c_{8x}$	0
									$d_{4x}^2c_{4x}^2$	0	$d_{4x}d_{4\theta}c_{4x}c_{4\theta}$	$d_{4x}d_{5x}c_{4x}c_{5x}$	0	$d_{4x}d_{6x}c_{4x}c_{6x}$	0	$d_{4x}d_{7x}c_{4x}c_{7x}$	0	$d_{4x}d_{8x}c_{4x}c_{8x}$	0
										$d_{4y}^2c_{4y}^2$	0	0	$d_{4y}d_{5y}c_{4y}c_{5y}$	0	$d_{4y}d_{6y}c_{4y}c_{6y}$	0	$d_{4y}d_{7y}c_{4y}c_{7y}$	0	$d_{4y}d_{8y}c_{4y}c_{8y}$
											$d_{4\theta}^2c_{4\theta}^2$	$d_{4\theta}d_{5x}c_{4\theta}c_{5x}$	0	$d_{4\theta}d_{6x}c_{4\theta}c_{6x}$	0	$d_{4\theta}d_{7x}c_{4\theta}c_{7x}$	0	$d_{4\theta}d_{8x}c_{4\theta}c_{8x}$	0
												$d_{5x}^2c_{5x}^2$	0	$d_{5x}d_{6x}c_{5x}c_{6x}$	0	$d_{5x}d_{7x}c_{5x}c_{7x}$	0	$d_{5x}d_{8x}c_{5x}c_{8x}$	0
			sym.										$d_{5y}^2c_{5y}^2$	0	$d_{5y}d_{6y}c_{5y}c_{6y}$	0	$d_{5y}d_{7y}c_{5y}c_{7y}$	0	$d_{5y}d_{8y}c_{5y}c_{8y}$
														$d_{6x}^2c_{6x}^2$	0	$d_{6x}d_{7x}c_{6x}c_{7x}$	0	$d_{6x}d_{8x}c_{6x}c_{8x}$	0
															$d_{6y}^2c_{6y}^2$	0	$d_{6y}d_{7y}c_{6y}c_{7y}$	0	$d_{6y}d_{8y}c_{6y}c_{8y}$
																$d_{7x}^2c_{7x}^2$	0	$d_{7x}d_{8x}c_{7x}c_{8x}$	0
																	$d_{7y}^2c_{7y}^2$	0	$d_{7y}d_{8y}c_{7y}c_{8y}$
																		$d_{8x}^2c_{8x}^2$	0
																			$d_{8y}^2c_{8y}^2$

MODEL VERIFICATION

Diaphragms tested in the laboratory were analyzed to verify our model. Descriptions of the diaphragms and test results were reported in a previous publication (Falk and Itani 1987). A total of ten wall, floor, and ceiling diaphragms were tested for ultimate load capacity. Single nail coupon tests were also performed to determine the properties of the fasteners used in the

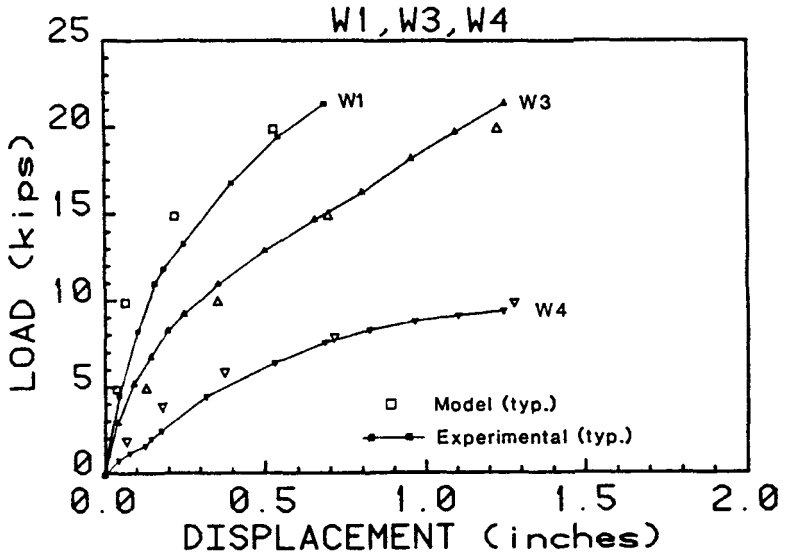

FIG. 5. Model and Test Results for Wall Diaphragm. Open Symbols Indicate Model Results; Closed Symbols Indicate Experimental Results

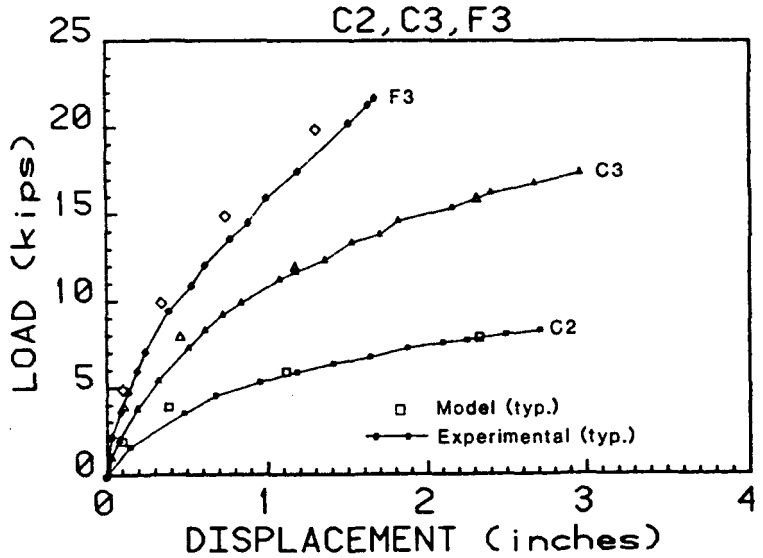

FIG. 6. Model and Test Results for Ceiling and Floor Diaphragms. Open Symbols Indicate Model Results; Closed Symbols Indicate Experimental Results

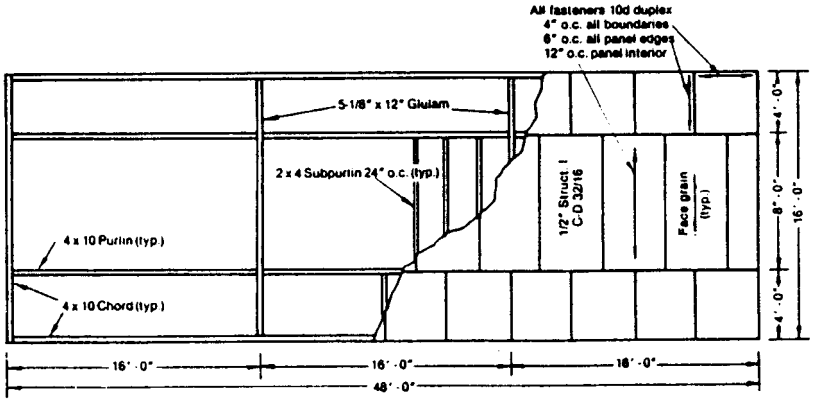

FIG. 7. 16 by 48 ft Diaphragm Tested by Tissell and Elliott (1977). (Figure Duplicated with Permission)

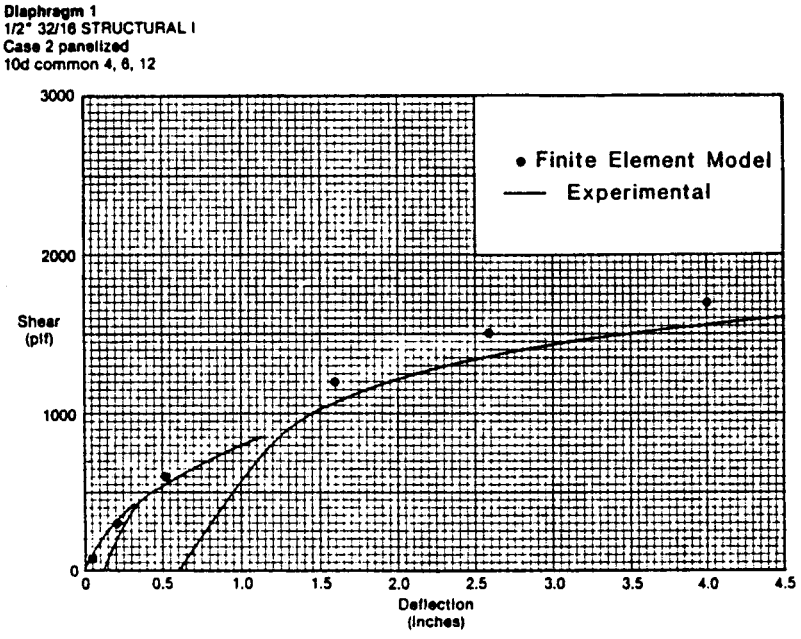

FIG. 8. Model and Test Results for 16 by 48 ft Diaphragm. (Figure Duplicated with Permission)

diaphragms. The load-displacement test results and model predictions for the tested wall diaphragms are shown in Fig. 5. Similar comparisons for ceiling and floor diaphragms are shown in Fig. 6. For the sake of clarity, not all diaphragms are shown. As illustrated in these figures, the model accurately predicted the response of the various types of diaphragms.

For practical reasons, the floor and ceiling diaphragms tested were subject to point loading. To verify the model for the case of uniform loading, we also analyzed a floor diaphragm tested by Tissell and Elliott (1977). This 16 by 48 ft diaphragm is shown in Fig. 7, and model and experimental

results are compared in Fig. 8. The finite element model predicted slightly lower values of displacement at higher loads than the values obtained experimentally. The 4- by 10-in chords of the diaphragm were spliced together with bolted connections at 16 ft intervals. The slip in these connections can be significant at higher diaphragm shear load levels. Because the model does not account for this chord splice slip, predicted displacements are expected to be somewhat less than measured values.

PARAMETRIC STUDIES

Using the verified model, sensitivity studies were performed to quantify the effect of various parameters on the load-displacement relationships of floor diaphragms. These parameters were nail modulus, nail spacing, framing properties, sheathing properties, and the effect of blocking. An evaluation of other parameters can be found in the cited reference (Itani and Falk 1987).

A 'standard" diaphragm (16 by 32 ft) was used in the parametric study (Fig. 9). In the analysis of this diaphragm, all joist and blocking connections were considered pinned. Note that unyielding supports were assumed along the width of the diaphragm. These support conditions were used to represent concrete or masonry support walls whose high rigidity resists out-of-plane twist. All displacement values presented correspond to the maximum deflection of the diaphragm at midspan.

Nail Modulus

Single-nail coupon tests were performed to determine the properties of the fasteners used in the tested diaphragms (Falk and Itani 1987). Nail modulus data points from 93 tests are shown in Fig. 10 along with a best fit curve of the data (solid line). To determine the effect of varying average nail prop-

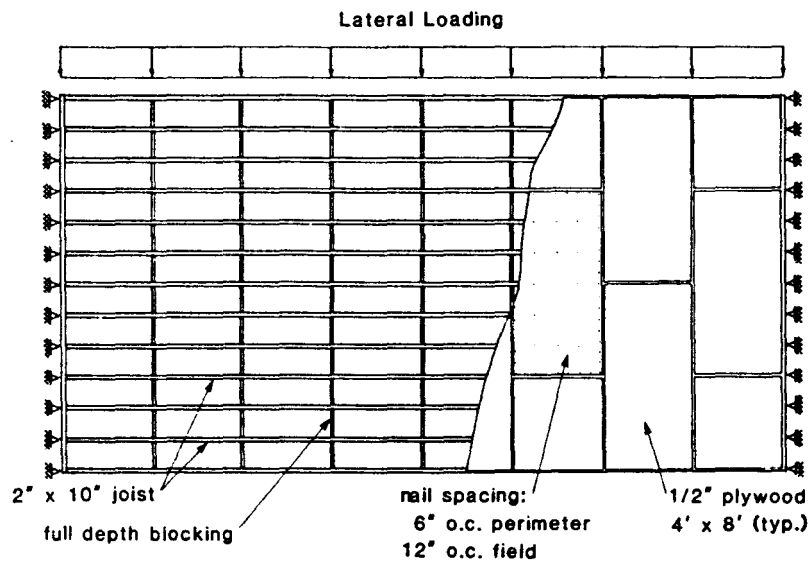

FIG. 9. "Standard" Diaphragm for Parametric Study

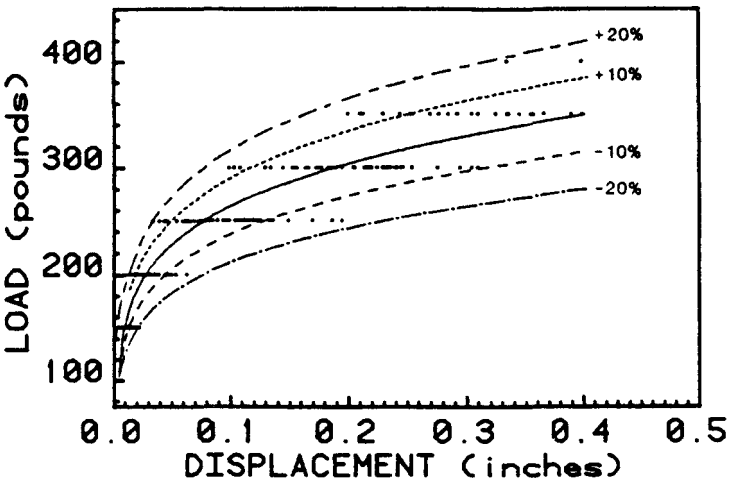

FIG. 10. Nail Modulus Results for Tests Using 1/2-in. Plywood and 6d Common Nails

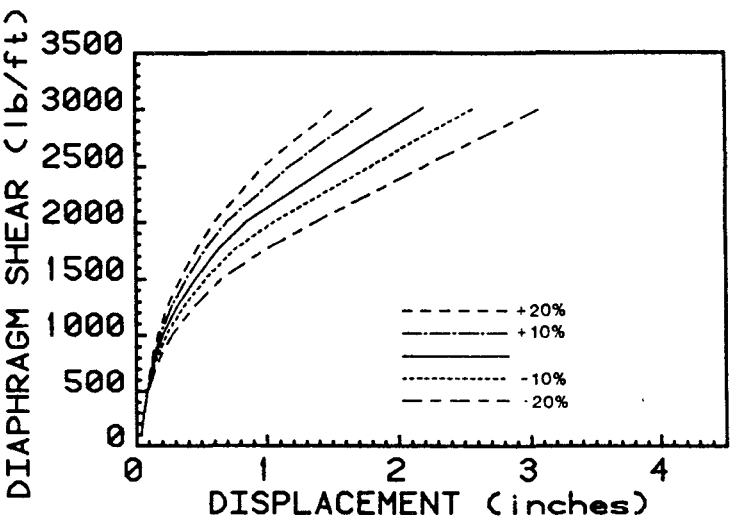

FIG. 11. Model Prediction of Diaphragm Displacement Caused by Variation in Nail Modulus

erties, the best fit curve was varied by ±10% and ±20%. Note that a variation of ±20% enclosed all data points. The ±20% curves are considered extremes in nail modulus behavior since these curves represent average values. Fig. 11 shows the results of the diaphragm lateral load analysis for this modulus variation.

If designed according to the Uniform Building Code, this standard floor diaphragm would be allowed to carry 185 lb/ft (International Conference of Building Officials 1985). For this reason, the relationship between stiffness and nail modulus variation was studied at this load level. As expected, the load-displacement results showed an increase in diaphragm stiffness as a

result of increasing the nail modulus. Conversely, diaphragm stiffness decreased as a result of a decrease in nail modulus. A 10% increase in nail modulus increased stiffness by about 4%, while a 20% increase of nail modulus increased stiffness 9%. Decreasing nail modulus by 10 and 20% caused a 4 and 9% decrease in stiffness, respectively.

This consistent variation in stiffness at the 185-lb/ft load level did not occur at higher diaphragm shear load levels. At a diaphragm shear load of 1,000 lb/ft, which is about five and a half times the allowable shear load, increasing the nail modulus by 10 and 20% resulted in a 12 and 22% increase in stiffness, respectively. However, a decrease by the same amounts resulted

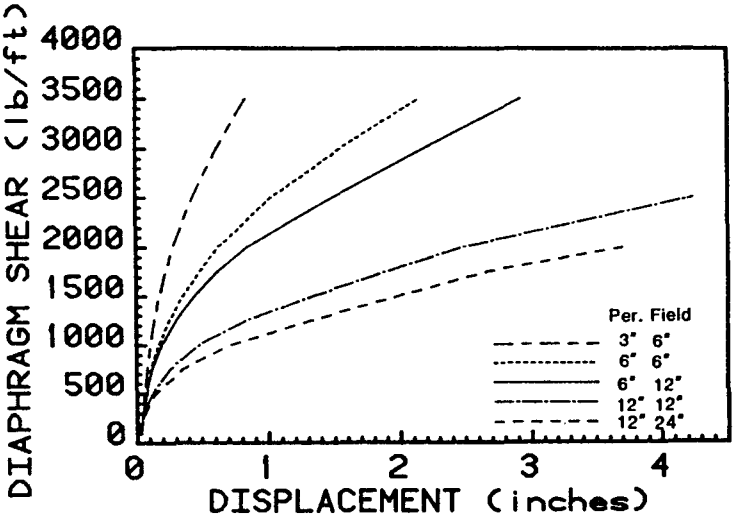

FIG. 12. Model Prediction of Diaphragm Displacement for Various Nail Spacings

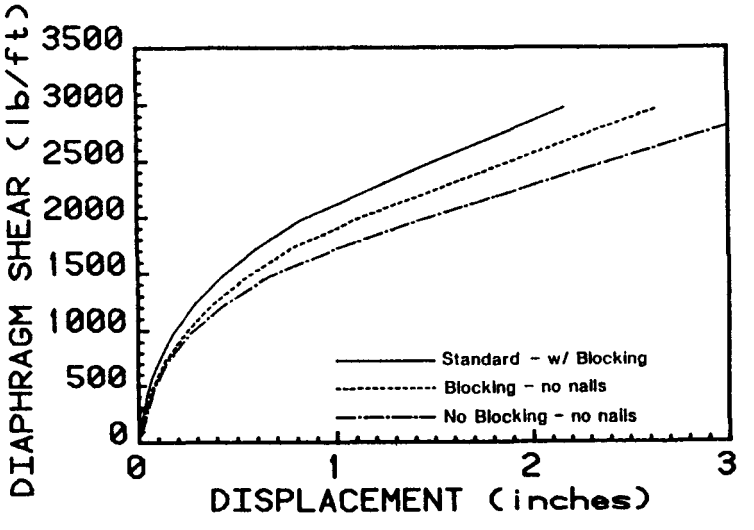

FIG. 13. Model Prediction of Diaphragm Displacement with and without Blocking

in a 19 and 40% decrease in stiffness, respectively. These variations were due to the nonlinear nature of the nail modulus curves.

Nail Spacing

The standard floor diaphragm was analyzed with various nail spacing to determine the effect of nail spacing on load-displacement characteristics. Standard nail spacing for each sheathing panel was assumed to be 6 in. on center (o.c.) for perimeter nails and 12 in. o.c. for field nails.

As shown in Fig. 12, a variance of perimeter nail spacing had a very dramatic effect on diaphragm stiffness; varying field nail spacing did not affect stiffness to the same extent. Experimental tests of walls have indicated similar trends (Easley et al. 1982).

At the 185-lb/ft shear load level, a decrease in perimeter and field nail spacing from 6 and 12 in. to 6 and 6 in., respectively, increased stiffness by only 4%. Further decreasing the perimeter and field nail spacing to 3 and 6 in., respectively, resulted in a 38% increase in diaphragm stiffness. Hence, the spacing of field nails had little effect on diaphragm stiffness. Increasing the perimeter and field nail spacings from 6 and 12 in. to 12 and 12 in., respectively, decreased stiffness by 31%, while increasing spacing to 12 and 24 in., respectively, decreased stiffness by 35%.

At the higher shear load level of 1,000 lb/ft, a decrease in the perimeter and field nail spacing from 6 and 12 in. to 6 and 6 in., respectively, resulted in a 13% increase in stiffness, while a decrease in perimeter and field nail spacing to 3 and 6 in., respectively, resulted in a 47% increase in stiffness. At this higher load level, an increase in nail spacing had a much more dramatic effect on stiffness. Increasing the perimeter and field nail spacing from 6 and 12 in. to 12 and 12 in., respectively, resulted in a 159% decrease in stiffness, while an increase to 12 and 24 in., respectively, decreased stiffness by nearly 300%.

Effect of Blocking

The use of blocking in a floor diaphragm is an important factor in determining how much shear load the diaphragm is allowed to carry (International Conference of Building Officials 1985). A blocked diaphragm benefits from the additional nails that secure the sheathing to the blocking as well as from the additional stiffness provided by frame action. The load-carrying capacity of a blocked diaphragm is typically limited by yielding of nail joints, nail pullout or pullthrough, and in the case of relatively thin sheathing (less than 1/2 in.), buckling of the sheathing. Unblocked diaphragms are more susceptible to sheathing buckling since the unblocked edges are not nailed.

The effect of blocking on the stiffness of the standard floor diaphragm was investigated by analyzing this diaphragm with blocking, with blocking but without blocking nails, and without blocking (no blocking nails) (Fig. 13). We were thus able to isolate how much stiffness was increased by the additional nails used with blocking and by the frame action caused by the use of blocking. At the 185-lb/ft allowable shear load level, stiffness of the standard diaphragm with blocking and without blocking nails was reduced about 16%, whereas removing both blocking and blocking nails reduced stiffness by 35%. Thus, the additional nails that secured the sheathing to the blocking and frame action had about an equal effect on diaphragm stiffness.

At the 1,000-lb/ft level, blocking without nails reduced stiffness about 34%, whereas removing both blocking and nails reduced stiffness by 49%. Thus, at higher load levels, the blocking was less effective in maintaining diaphragm stiffness.

CONCLUSIONS

The finite element model presented in this report can be used to analyze the nonlinear load displacement of wood diaphragms. Various geometries, sheathing types, and fastener spacings can be investigated with this model.

A comparison of model results with experimental test results indicates that our model can predict diaphragm response. Parametric studies determined the dominant effects of nail properties and nail spacing on diaphragm stiffness. At the allowable diaphragm shear load levels investigated, a variation of ±20% in nail modulus increased or decreased diaphragm stiffness by less than 10%. Since these variations in nail load-slip are considered extremes, the effect of nail modulus on stiffness was not significant. Nail spacing had a greater effect on diaphragm stiffness than nail modulus. Stiffness was more affected by perimeter nail spacing than field nail spacing. Blocking increased diaphragm stiffness; this increase was caused by both the greater number of nails used with blocking and the increased frame action provided by blocking.

ACKNOWLEDGMENTS

The research reported in this paper was carried out at Washington State University and sponsored by the National Science Foundation under contract CEE 830121. Findings and conclusions expressed in this paper are those of the writers and do not necessarily reflect the view of the National Science Foundation.

The assistance provided by Drs. Chung K. Cheung and Fumio Kamiya is gratefully appreciated.

APPENDIX I. REFERENCES

Amana, E. J., and Booth, L. G. (1967). "Theoretical and experimental studies of nailed and glued plywood stress-skinned components: Part 1, theoretical study." *J. Inst. Wood Sci.*, 4(1), 43–69.

Cheung, C. K. (1984). "NONDIA—A structural analysis program for the static and dynamic response of nonlinear nailed wood diaphragm systems (modified from NONSAP)." *Dept. of Civ. Engrg.*, Washington State University, Pullman.

Easley, J. T., Foomani, M., and Dodds, R. H. (1982). "Formulas for wood shear walls." *J. Struct. Engrg.*, ASCE, 108(11), 2460–2478.

Falk, R. H., and Itani, R. Y. (1987). "Dynamic characteristics of wood and gypsum diaphragms." *J. Struct. Engrg.*, ASCE, 113(6), 1357–1370.

Foschi, R. O. (1977). "Analysis of wood diaphragms and trusses. Part I: Diaphragms." *Can. J. Civ. Engrg.*, 4(3), 345–352.

Gupta, A. K., and Kuo, G. P. (1985). "Behavior of wood-framed shear walls." *J. Struct. Engrg.*, ASCE, 111(8), 1722–1733.

Gupta, A. K., and Kuo, G. P. (1987). "Wood framed shear walls with uplifting." *J. Struct. Engrg.*, ASCE, 113(2), 241–259.

International Conference of Building Officials. *Uniform Building Code*, 1985 edition, Whittier, Calif.
Itani, R. Y., and Cheung, C. K. (1984). "Nonlinear analysis of sheathed wood diaphragms." *J. Struct. Engrg.*, ASCE, 110(9), 2137–2147.
Itani, R. Y., and Falk, R. H. (1986). "Damage and collapse behavior of lowrise wood-frame buildings: Diaphragms." Final report to the National Science Foundation in fulfillment of grant CE830121, Washington State University, Pullman, Wash., Dec.
Kallsner, B. (1983). "Windaussteifung von wandkonstruktionen in holzskelettbau mit plattenwerkstoffen" ("Wind stiffening of wall constructions in wood-skeleton structures with plate materials"). *Bauen mit Holz*. June, 374–377, (in German).
Kamiya, F. (1981). "Theoretical studies on racking stiffness and strength of wooden sheathed walls." *Trans. Architect. Inst. Japan*, Report No. 309, Nov..
Kamiya, F., Hirashima, Y., and Hatayama, Y. (1983). "Studies on wood panel construction (II): Evaluation of a shear wall by analytical method." *Bull. Forestry For. Prod. Res. Inst.*, Report No. 332, Japan.
McCutcheon, M. (1985). "Racking deformations in wood shear walls." *J. Struct. Engrg.*, ASCE, 111(2), 257–269.
Petersen, J. (1983). "Bibliography on lumber and wood panel diaphragms." *J. Struct. Engrg.*, ASCE, 109(12), 2838–2852.
Tissel, J. R., and Elliott, J. R. (1977). "Plywood diaphragms." Research Report 138. Am. Plywood Assoc., Tacoma, Wash.
Tuomi, R. L., and McCutcheon, W. J. (1978). "Racking strength of light frame nailed walls." *J. Struct. Div.*, ASCE, 104(7), 1131–1140.

APPENDIX II. NOTATION

The following symbols are used in this paper:

a = location of spring pair as a ratio of its y coordinate and transfer element height;
b = location of spring pair as a ratio of its x coordinate and transfer element width;
c = functions describing spring pair displacement in terms of element width;
d = functions describing spring pair displacement in terms of element height;
f = spring pair force;
H = element height;
k = spring pair stiffness;
m = total number of spring pairs in row;
n = total number of spring pairs in column;
K_e = transfer element stiffness;
S = nodal force;
W = element width;
(x) = x coordinate; and
(y) = y coordinate.

Subscripts

Subscripted numbers refer to nodes.
i = ith spring pair in a row;
j = jth spring pair in a column; and
x, y, θ = direction of force or unit displacement.